Cell Reports Medicine, Volume *5*

Supplemental information

The impact of bed rest on human skeletal muscle metabolism

Moritz Eggelbusch, Braeden T. Charlton, Alessandra Bosutti, Bergita Ganse, Ifigenia Giakoumaki, Anita E. Grootemaat, Paul W. Hendrickse, Yorrick Jaspers, Stephan Kemp, Tom J. Kerkhoff, Wendy Noort, Michel van Weeghel, Nicole N. van der Wel, Julia R. Wesseling, Petra Frings-Meuthen, Jörn Rittweger, Edwin R. Mulder, Richard T. Jaspers, Hans Degens, and Rob C.I. Wüst

Table S1. Effect of antigravitation intervention on outcome measures. Related to STAR Methods participant recruitment, Figures 1 and 5. The continuous or intermittent anti-gravitational interventions (cAG, 30 minutes daily and iAG, 6x5 minutes daily) did not mitigate the bed rest-induced alterations in HOMA2-IR scores, or oxidative phosphorylation (OXPHOS) capacity of the skeletal muscle. All data were analyzed by repeated measures ANOVA, mixed-effects model with Tukey's post hoc test, n=24 for each parameter. HOMA2-IR: homeostatic model assessment (HOMA) for insulin resistance.

	HOMA2-IR				
	Control	cAG (30')	iAG (6x5')	Total	*p*
Day 0	0.64 ± 0.15	0.52 ± 0.10	0.53 ± 0.22	0.56 ± 0.07	0.52
Day 6	1.04 ± 0.32	0.76 ± 0.13	0.66 ± 0.23	0.82 ± 0.20	0.13
Day 55	0.99 ± 0.43	0.80 ± 0.13	0.65 ± 0.22	0.81 ± 0.17	0.35
	OXPHOS capacity				
	Control	cAG (30')	iAG (6x5')	Total	*p*
Day 0	81 ± 15	75 ± 19	69 ± 22	75 ± 6	0.47
Day 6	80 ± 21	66 ± 12	65 ± 13	70 ± 9	0.12
Day 55	58 ± 8	64 ± 16	49 ± 10	57 ± 8	0.11

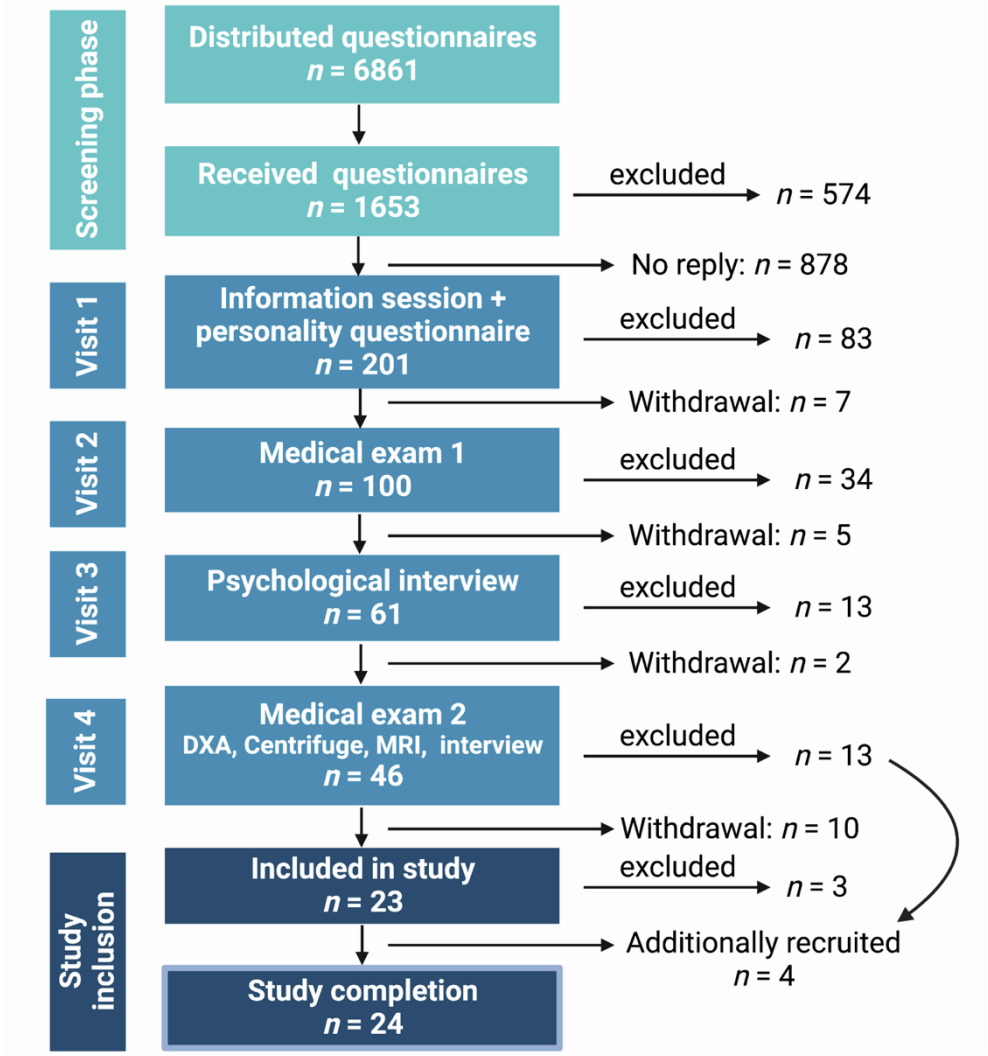

Figure S1. Participant screening process. Related to STAR Methods participant recruitment. Out of 6861 distributed questionnaires, 1653 potential participants received further information, and 201 people joined an on-site visit and assessment at the German Aerospace Centre. Three subsequent on-site visits included more rigorous assessments, and 23 healthy participants were initially included in the study. Three participants were excluded and replaced by four participants on the reserve list.

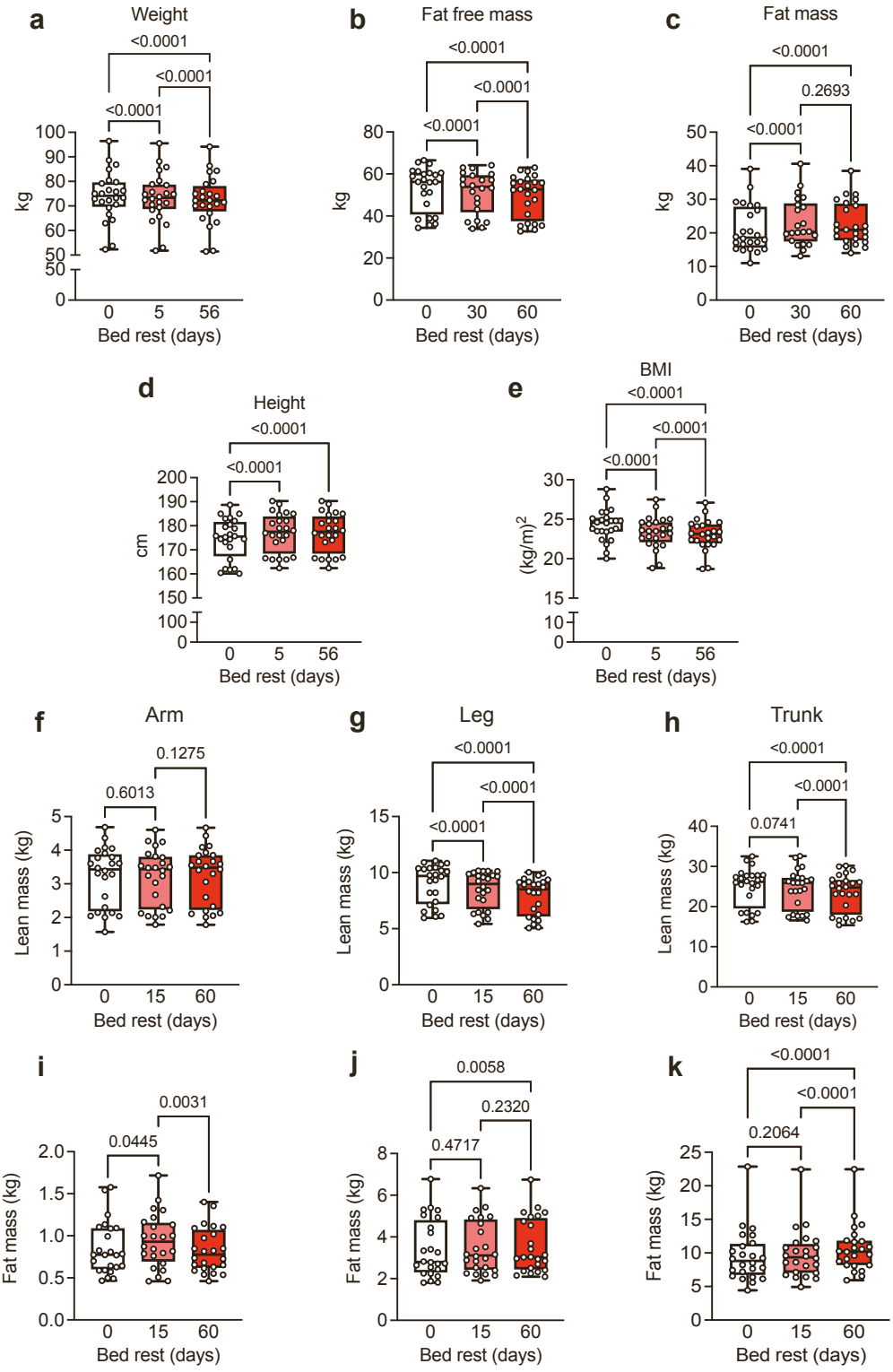

Figure S2. Bed rest decreases BMI, but increases trunk and leg body fat. Related to Figure 1. a-d: Participant body weight (**a**) and fat free mass (**b**) decreased throughout the bed rest. While fat mass progressively increased (**c**), and height increased (**d**), body mass index (**e**) decreased during bed rest. **f-g:** Arm lean mass remained unchanged throughout the bed rest (**f**), whereas leg (**g**) and trunk lean mass (**h**) decreased progressively throughout the bed rest. Arm fat mass (**i**) transiently increased after 15 days, but decreased to pre-bed rest values after 60 days. Leg (**j**) and trunk fat mass (**k**) increased following 60 days of bed rest. Analysis with repeated measures ANOVA, with Tukey's post hoc test, *n*=24.

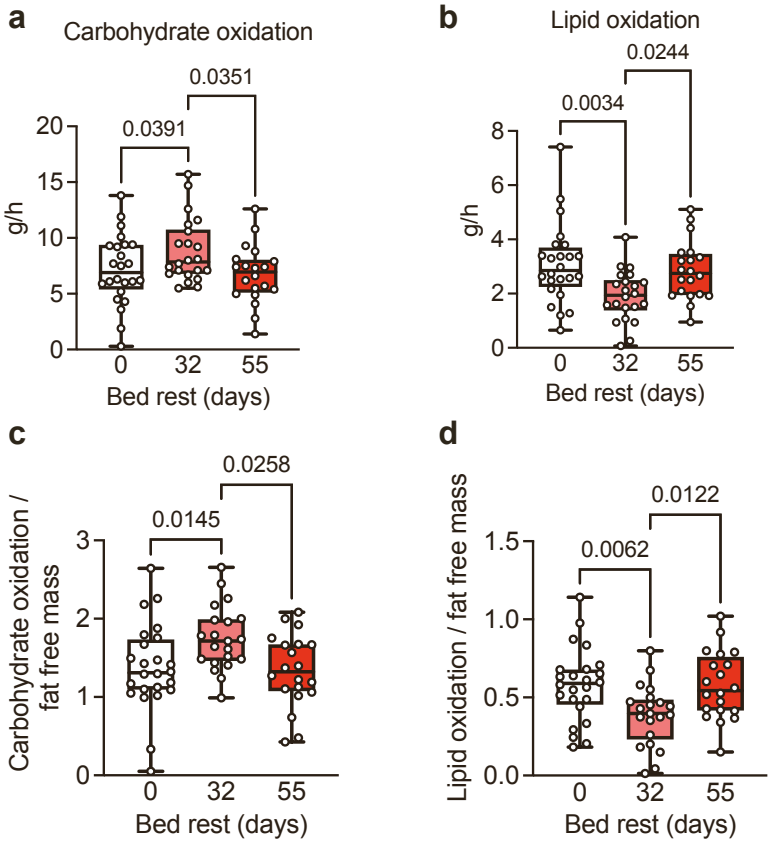

Figure S3. Bed rest alters fasted resting substrate oxidation. Related to Figure 1. a-b: Resting carbohydrate oxidation in the fasted state (**a**) increased after 32 days of bed rest, while lipid oxidation transiently decreased (**b**), and reduced to pre-bed rest values after 55 days. **c-d:** Time courses of substrate oxidation were similar after normalization for fat free mass. Analysis with repeated measures ANOVA, with Tukey's post hoc test, *n*=24.

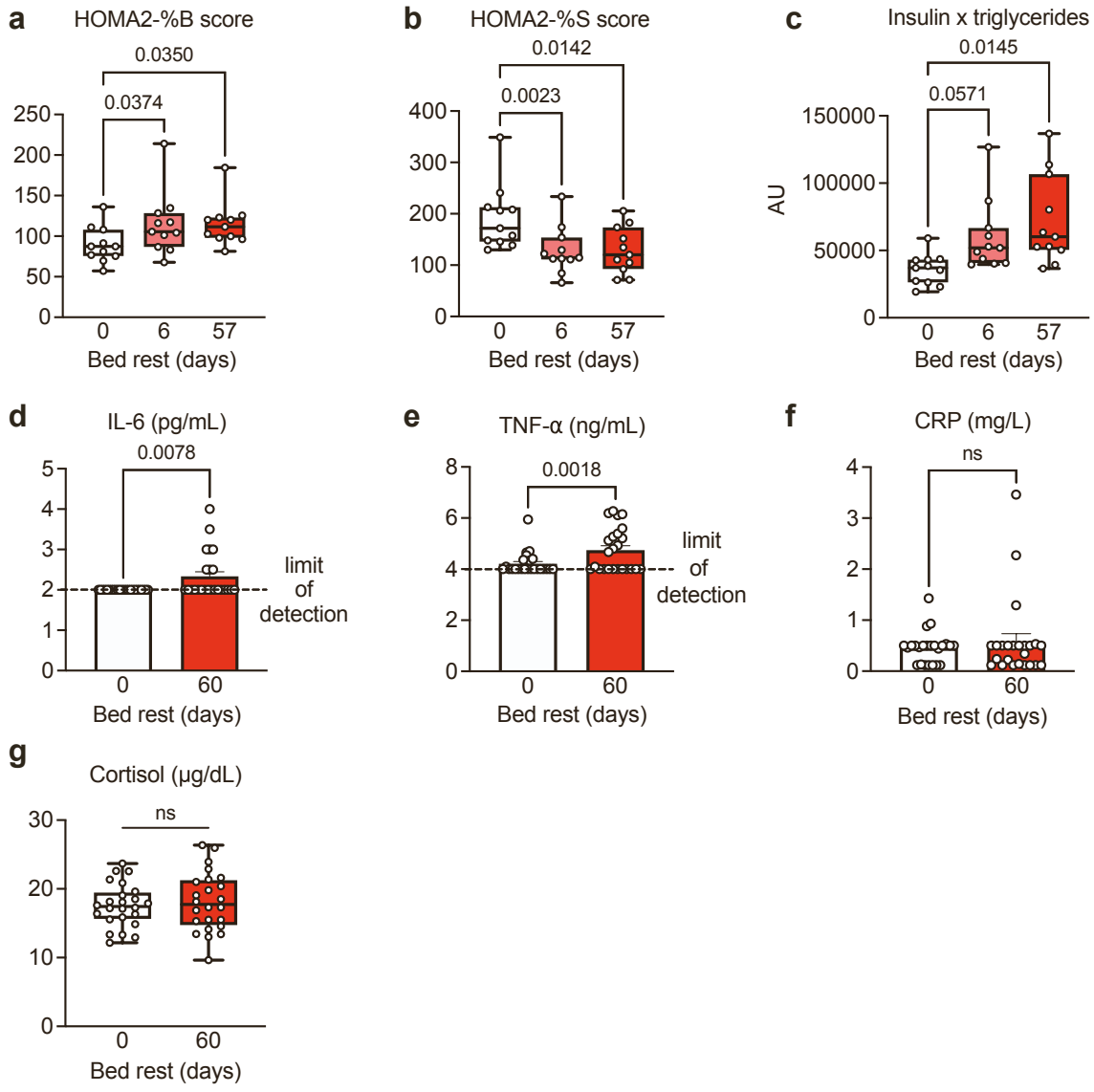

Figure S4. Bed rest acutely impairs insulin sensitivity and increases circulating pro-inflammatory cytokines after long-term bed rest while stress levels remain unchanged. Related to Figure 1. a: HOMA2-%B, indicative of pancreatic β-cell function, increased after short-term and long-term bed rest. **b:** HOMA2-%S reduced after short- and long-term bed rest, indicative of a reduced insulin sensitivity. **c**: The product of systemic insulin and plasma triglyceride levels as an indirect marker for adipose tissue insulin resistance (adipo-IR) increased after bed rest. **d-g:** Inflammatory markers IL-6 (**d**) and TNF-**α** (**e**) increased significantly after long-term bed rest, whilst C-reactive protein (**f**) and cortisol levels (**g**) remained unchanged. Analysis with repeated measures ANOVA, with Tukey's post hoc test, *n*=12 for panel a-c, Wilcoxon matched-pairs rank test for panel d-f, paired *t*-test for panel g, *n*=24 for stress and inflammation markers.

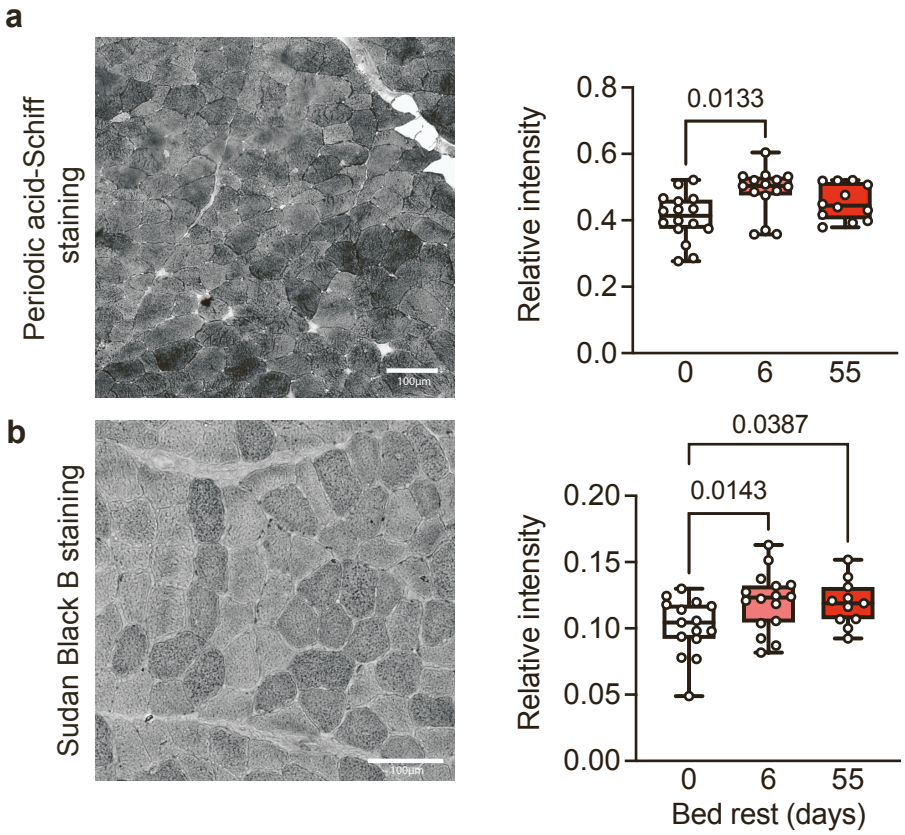

Figure S5. Bed rest-induced nutrient overload. Related to Figure 2. a: Typical example and relative optical densities of a Periodic acid-Schiff (PAS) staining, performed in muscle sections to measure glycogen concentrations according to staining intensity, showed increased glycogen accumulation after short-term bed rest. **b**: A Sudan Black B staining was performed to study intra- and extracellular lipid accumulation after short- and long-term bed rest. Intracellular lipid accumulation increased after bed rest, but no signs of extracellular lipid accumulation (intermuscular adipose tissue) were observed. PAS data were analysed by Kruskal-Wallis test, with Dunn's post-hoc test, as data were not normally distributed, *n*=12-16. Due to missing values, Sudan Black B data were analysed with a one-way ANOVA with Fisher's LSD, *n*=11-16. Scale bar=100µm.

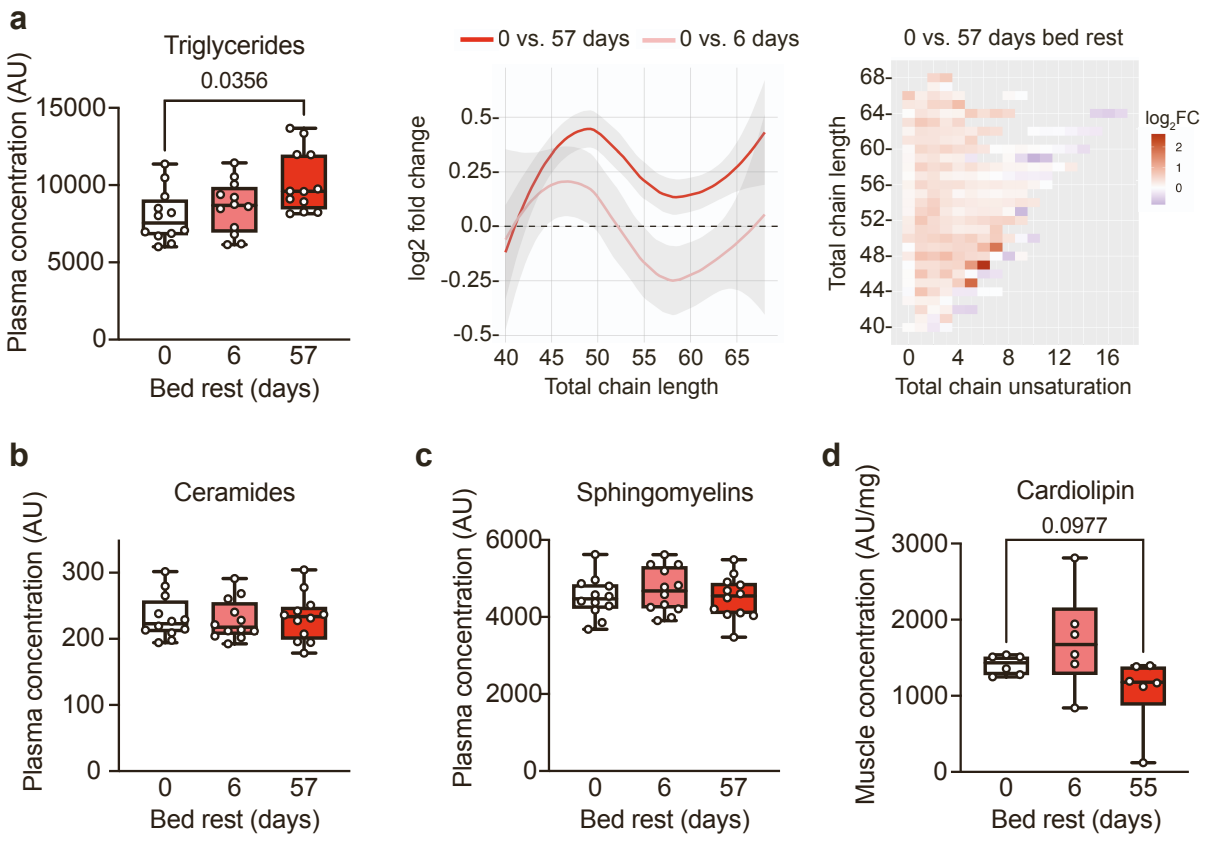

Figure S6. Blood lipidomics show few changes with short- and long-term bed rest. Related to Figure 3. Mass-spectrometry based lipidomics analysis using blood plasma collected throughout the bed rest. Out of 1402 identified lipid species, 243 were significantly altered after short- (95 downregulated) and 160 lipids changed significantly (64 downregulated) after long-term bed rest. **a:** Plasma triglyceride concentrations increased significantly after long-term bed rest, at all chain lengths, particularly at low chain unsaturations**.** Blood plasma ceramide (**b**) and sphingomyelin (**c**) concentrations did not change throughout the bed rest period. No differences were observed in other lipid classes in the blood plasma. Cardiolipin concentration in the skeletal muscle tended to be lower after long-term bed rest (**d**). Concentrations were analysed using repeated measures ANOVA, with Tukey's post hoc test, *n*=12 for plasma, *n*=6 for muscle.

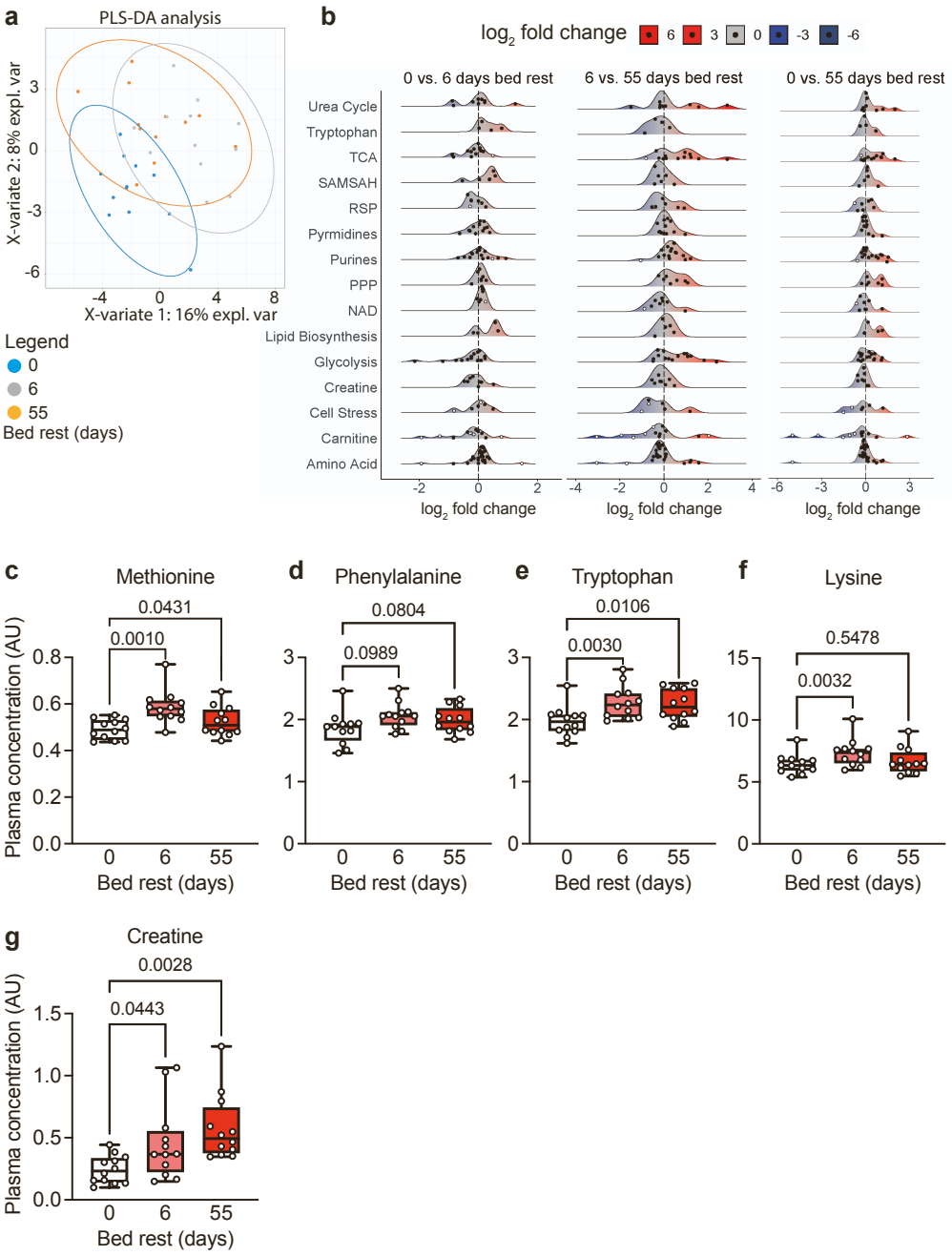

Figure S7. Blood plasma metabolomics upon bed rest. Related to Figure 4. a-b: Landscape plots of plasma metabolomics analysis, mapping the metabolic response in blood plasma upon short- and long-term bed rest. White dots represent significantly altered (p<0.05) metabolites. Metabolite concentration shifts are presented as log_2 fold changes to indicate directionality of alterations. **c-g:** The differential response in the circulating branched-chain amino acids methionine (**c**), phenylalanine (**d**), tryptophan (**e**), lysine (**f**), and circulating creatine concentrations (**g**) upon short- and long-term bed rest is possibly due to increased muscle breakdown. Concentration changes of individual metabolites were analysed using repeated measures ANOVA, with Tukey's post hoc test, n=12. TCA: tricarboxylic acid cycle; SAMSAH: S-adenosylmethionine/S-adenosylhomocysteine cycle; RSP: reductive stress panel; PPP: pentose phosphate pathway; NAD: Nicotinamide adenine dinucleotide pathway.

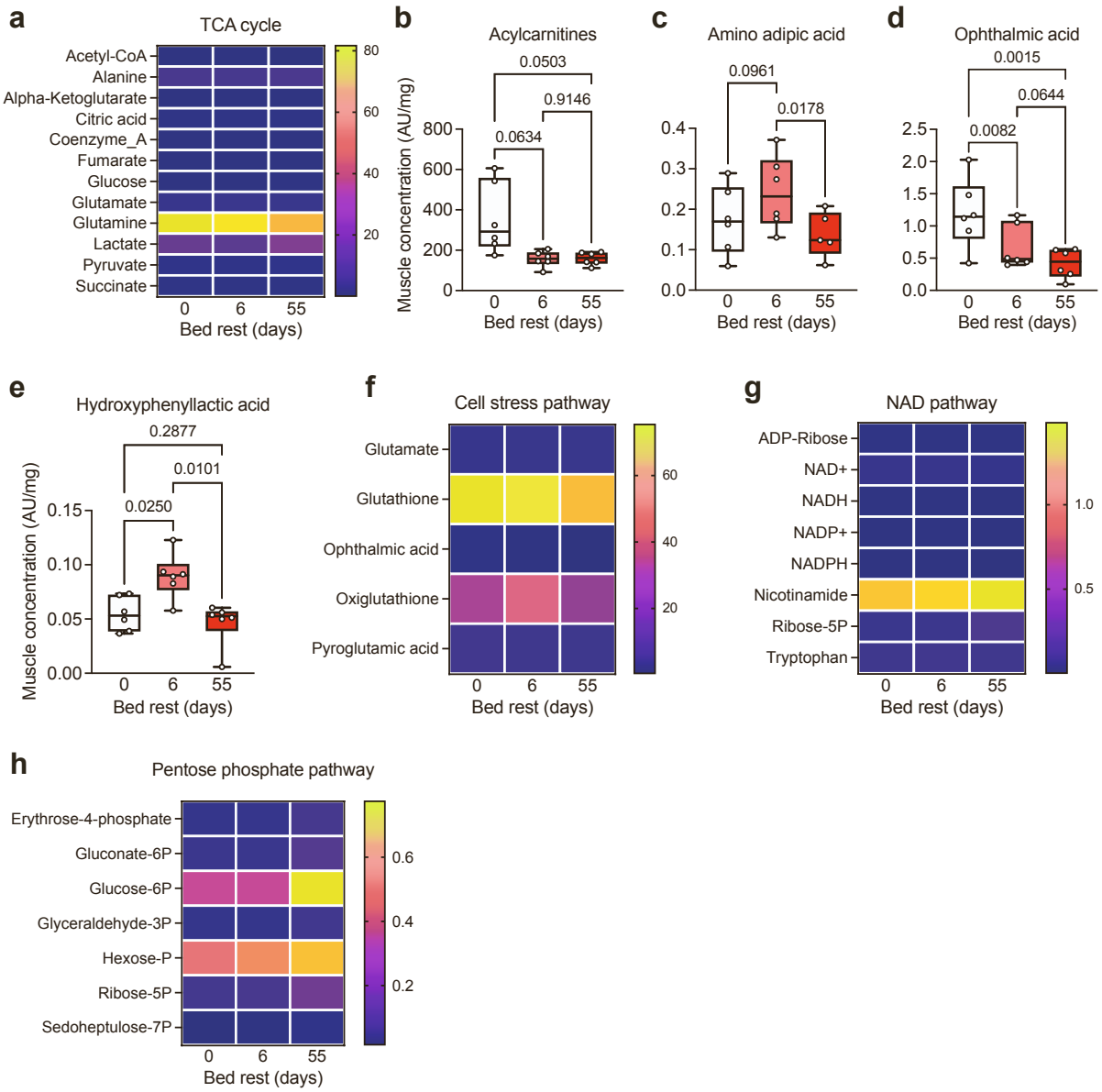

Figure S8. Muscle metabolomics confirm a bed rest-induced metabolic shift towards glucose metabolism in skeletal muscle. Related to Figure 4. a: Heat map of metabolites related to the TCA cycle show less glutamine upon long-term bed rest. **b**: Total acylcarnitines were significantly reduced after short-term bed rest and remained reduced after long-term bed rest. **c-e**: Changes in skeletal muscle, amino adipic acid (**c**), opthalmic acid (**d**) and hydroxyphenyllactic acid (**e**) over the course of the bed rest. **f-h**: Heat maps of metabolites related to cell stress (**f**), the NAD^+ pathway (**g**), and the pentose phosphate pathway (**h**) upon short- and long-term bed rest. Concentration changes of individual metabolites were analysed using repeated measures ANOVA, with Tukey's post hoc test, *n*=6. TCA: tricarboxylic acid cycle

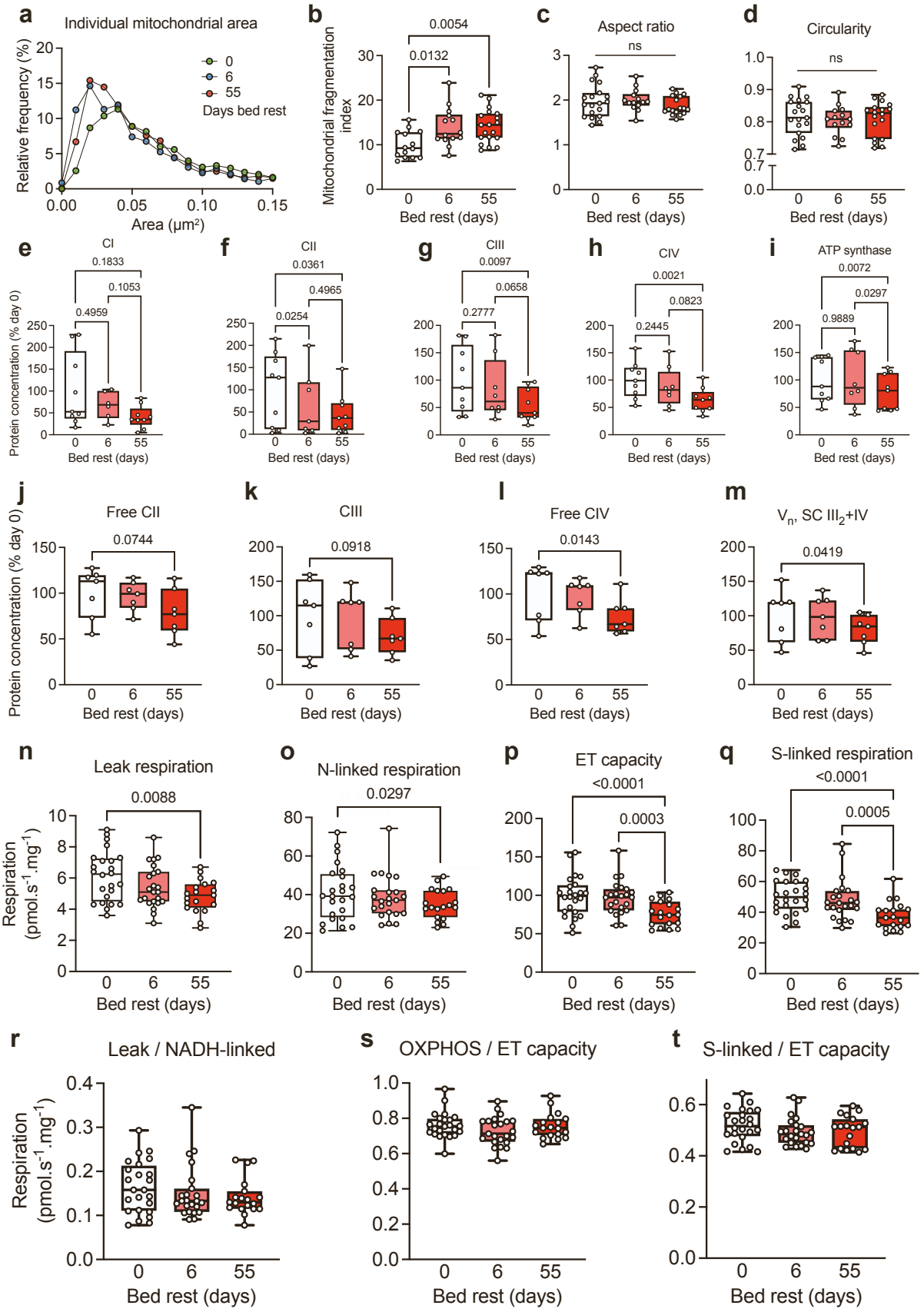
a
Individual mitochondrial area
Relative frequency (%)
Area (µm²)
0
6
55
Days bed rest
b
Mitochondrial fragmentation index
0.0054
0.0132
Bed rest (days)
c
Aspect ratio
ns
d
Circularity
ns
e
CI
0.1833
0.1053
0.4959
Protein concentration (% day 0)
f
CII
0.0361
0.4965
0.0254
g
CIII
0.0097
0.0658
0.2777
h
CIV
0.0021
0.0823
0.2445
i
ATP synthase
0.0072
0.0297
0.9889
j
Free CII
0.0744
k
CIII
0.0918
l
Free CIV
0.0143
m
Vn, SC III2+IV
0.0419
n
Leak respiration
0.0088
Respiration (pmol.s-1.mg-1)
o
N-linked respiration
0.0297
p
ET capacity
<0.0001
0.0003
q
S-linked respiration
<0.0001
0.0005
r
Leak / NADH-linked
s
OXPHOS / ET capacity
t
S-linked / ET capacity

Figure S9. Alterations in mitochondrial structure and function upon bed rest. Related to Figure 5. a-b: A left-shift of the relative frequency distribution after short- and long-term bed rest (**a**) indicates a reduction in individual mitochondrial size, confirmed by an increase in the mitochondrial fragmentation index (**b**) calculated as the total mitochondrial number divided by total mitochondrial area. **c-d:** Mitochondrial aspect ratio (**c**) and circularity (**d**) did not change upon bed rest. **e-i:** Individual protein concentrations of subunits of the mitochondrial complexes were reduced after long-term, but not short-term bed rest. **j-m**: While the abundance of mitochondrial supercomplexes decreased upon bed rest (Figure 5), also the free complex II, III and IV decreased. The abundance of mitochondrial supercomplex III_2+IV decreased after long-term bed rest. **n-q**: Leak and NADH-linked respiration, electron transfer (ET) capacity, and succinate-linked respiration only decreased after long- but not short-term bed rest. **r-t:** Respiratory control ratios did not alter throughout the bed rest period. Data were analysed using repeated measures ANOVA, with Tukey's post hoc test, n=14-19 for mitochondrial morphology, n=9 for immunoblotting, n=7 for BN-PAGE, n=24 for respirometry.